

MODELING STUDY OF CARBONATION MECHANISMS OF CO₂-CaO AND CO₂-NaOH REACTIONS

Mustafa Abunowara¹ and Mohamed Elgarni¹

Abstract: Calcium oxide (CaO) and sodium hydroxide (NaOH) have been used among various solid sorbents for CO₂ capture. Therefore, it is necessary to study the major controlling steps between the reactions of CO₂ and solid sorbents. The CO₂ uptake and the rate constant of the CO₂-CaO and CO₂-NaOH reactions were investigated using atmosphere thermogravimetric analyzer (ATGA) to understand its reaction mechanisms and speed span. A shrinking core model was utilized to determine the rate controlling steps, mass transfer coefficient, diffusion coefficient, and the time for complete conversion of a particle at ash diffusion controls regime. The results have been shown that the time for complete conversion of CaO and NaOH particles is chemical reaction controls regime for carbonation cycle. The chemical reaction was found to be the major controlling step reaction at initial minutes. After that the product layer diffusion became gradually more dominant controlling step in CO₂-CaO and CO₂-NaOH reactions. Therefore, the results been shown that diffusion mechanism is the main dominant regime for the remaining reaction cycle. These outcomes contribute to the understanding of how CO₂ reacts with CaO and NaOH solid sorbents at various temperature ranges.

Keywords: CO₂ sorption; CaO carbonation; NaOH; Shrinking core model; Thermogravimetric analyzer.

INTRODUCTION

Carbon dioxide (CO₂) emissions have been increased into atmosphere due to the combustion of fossil fuels, resulting in adverse impacts on the earth environment such as global warming, increasing sea level and climate change (Lin *et al.*, 2021). According to the Intergovernmental Panel on Climate (IPCC), carbon emissions will raise without any intervention from 36Gt/yr to between 48 and 55Gt/yr by 2050 with the continuous increase of energy demand (Pachauri *et al.*, 2014). The CO₂ concentration for 2100 on current trend will reach 530-980 ppm, possibly doubling the present level of ~410ppm and much higher than the preindustrial level of 280ppm. To avoid the apparent mean temperature rise caused by the rapid accumulation of CO₂, active removal of CO₂ is highly demanded (Hu *et al.*, 2021). Extensive research has been dedicated recently to CO₂ capture technologies due to growing

concerns with respect to greenhouse gases emissions (Breidenich *et al.*, 1998; Huaman *et al.*, 2014; Aydin *et al.*, 2010; Abunowara *et al.*, 2020 and Suleman *et al.*, 2020). CO₂ capture efficiency is the main challenge, where the core technology involves the usage of adsorption materials. Such as porous polymer-based solid amine adsorbents, fiber-based solid amine adsorbents, and thermo-responsive adsorbents have been developed for CO₂ capture. CO₂ adsorbents such as porous carbons and metal-organic frameworks particularly involve physical adsorption as the main CO₂ adsorption mechanism, where the adsorption characteristics specifically depend on the pore volume (Lin *et al.*, 2021). However, non-catalytic fluid solid reactions are common occurrence in chemical and metallurgical industries, pollution abatement (Bhattacharya and Purohit, 2004). Calcium based materials have attracted particular attention as potential sorbents for cyclic CO₂ capture processes. Among the possible applications of calcium based sorbents for CO₂ removal are steam reformers, gasifies of fossil fuels to enhance water-gas-shift reaction giving high hydrogen yields, and fluidized bed

¹Libyan Petroleum Institute (LPI) Tripoli, Libya.
E-mail address: abunowara1980@gmail.com,
mohamed.elgarni@cnrl.com

combustors with *in situ* CO₂ capture. These applications all involve sorbent cycling between calcination and carbonation (Sun *et al.*, 2008a). The CO₂-CaO and CO₂-NaOH reactions are growing interest because of their potential usefulness and high affinity in CO₂ capture in such industrial systems as steam reformers, gasifiers and fluidized bed combustors (Sun *et al.*, 2008b).

As a typical gas-solid reaction producing a solid product, carbonation is initially fast, followed by a much slower stage (Barker, 1973; Bhatia & Perlmutter, 1983; Abanades & Alvarez, 2003 and Alvarez & Abanades, 2005). An intrinsic kinetic study for the CaO-CO₂ reaction with a wide range of CO₂ partial pressure was tested using both atmosphere thermogravimetric analyzer (ATGA) and pressurized thermogravimetric analyzer (PTGA). It has been found that the intrinsic rate have a variable order with respect to CO₂ partial pressure. It was initially first-order reaction changing to zero-order and dependence when the CO₂ partial pressure exceeded ~10kPa (Sun *et al.*, 2008a & b).

Non catalytic reaction of particles with surrounding fluid, there are several models in which two of them which are characterized as simple idealized models namely, progressive-conversion and shrinking unreacted-core models which are considered for studying the carbonation cycles. For instance, progressive-conversion model (PCM) the reactant gas enters and reacts throughout the particle at all times, most likely at various rates and at various locations within the particle. Solid reactant is converted continuously and progressively throughout the particle. While, in the shrinking-core model (SCM), the reaction occurs first at the outer layer of the particle and the zone of reaction then moves into the solid matrix. As result, leaving behind completely converted material and inert solid and this considered as "ash". At any time there exists an unreacted core of material which shrinks in size during reaction (Levenspiel, 1999).

In this study, thermogravimetric analyzer (TGA) has been utilized to measure CO₂ sorption on CaO and NaOH solid sorbents at various temperature ranges. The results of CO₂ sorption on CaO and NaOH solid sorbents have been investigated using shrinking core model to understand how CO₂ molecules interact with the sorbent matrix. The kinetic model has been utilized to determine the rate controlling steps,

mass transfer coefficient, diffusion coefficient, and the time for complete conversion of a particle at ash diffusion controls regime. Therefore, this paper focuses on studying rate controlling steps for the CaO-CO₂ and CO₂ NaOH reactions at various temperature ranges.

EXPERIMENTAL PROCEDURE

The *Labsys* TG SETARAM instrument has been used in thermal analysis and calorimetry for gas solid reactions and in thermal degradation process. Thermal gravimetric analyzer (TGA) instrument has been utilized in this study to record the mass uptake of the samples when exposed to carbon dioxide atmosphere. A schematic diagram of TGA apparatus is shown in (Fig. 1). The reactivity testing of calcium oxide (CaO) and caustic soda (NaOH) sorbents for carbonation processes has been carried out separately in the TGA apparatus. A small sample of the sorbent (65mg) was placed in a platinum crucible and the weight of the sample was recorded progressively at every second. The scanning rate was maintained at 10°C/min. First precursor was calcium carbonate; the furnace temperature raised from 30°C to 1000°C then started the decarbonation cycle for CaCO₃ to assure that the material (calcium carbonate) fully decomposed to CaO. After that the instrument started cooling down until it reaches the required temperature and after that the isotherm cycle directly started for one hour, hence finishing the decarbonation and isotherm cycles under nitrogen gas (N₂) then switch to carbon dioxide gas to begin the carbonation cycle for three hours and the temperature ranges were used in study between (550-750°C). The second material was caustic soda (NaOH). The furnace temperature was raised from 30°C to the required temperature ranges between (75-225°C) then the furnace started automatically heating under the isotherm cycle for half hour. The heating and isotherm cycles performed under nitrogen gas (N₂) then directly switch to carbon dioxide gas (CO₂) to begin the carbonation cycle for one hour.

Modelling of Carbonation Reactions

Shrinking-Core Model

This model was first developed by (Yagi and Kunii, 1955 & 1961) who visualized five steps occurring in succession during reaction:

1. Diffusion of gaseous reactant (A) through the film surrounding the particle to the surface of the solid.

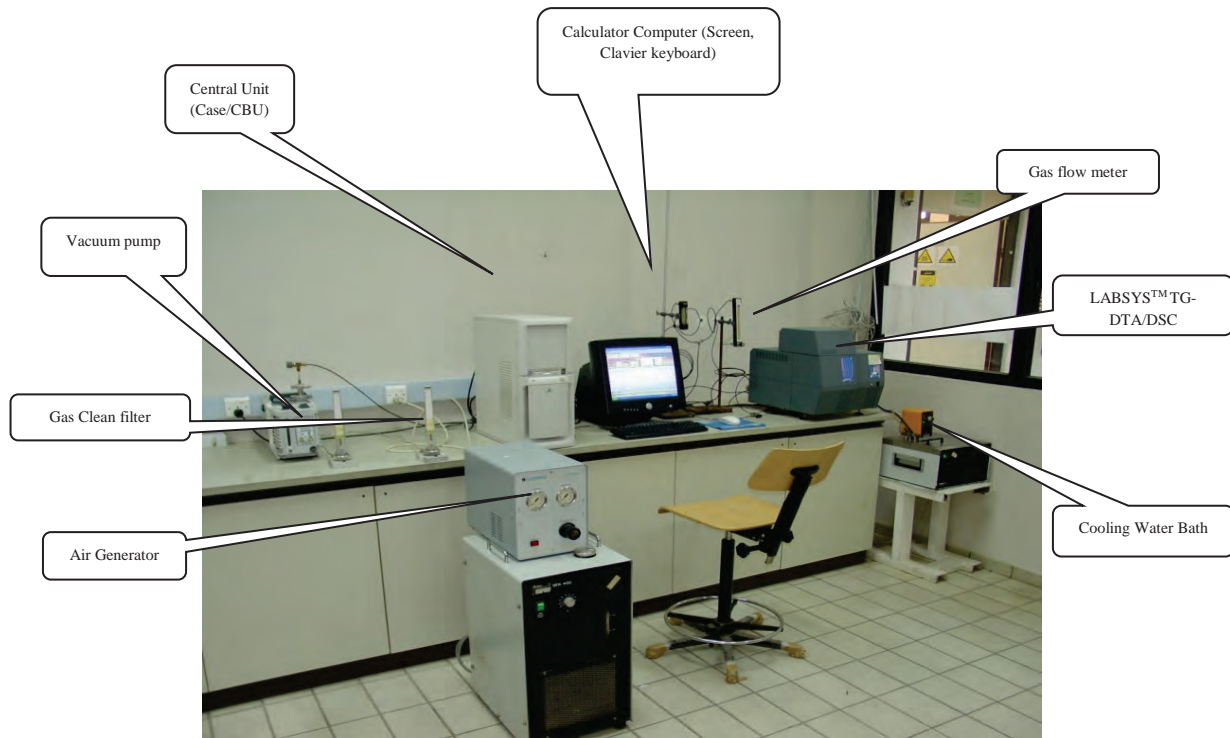


Fig. 1. Schematic of TGA apparatus

2. Penetration and diffusion of (A) through the blanket of ash to the surface of the unreacted core.
3. Reaction of gaseous (A) with solid at this reaction surface.
4. Diffusion of gaseous products through the ash back to the exterior surface of the solid.
5. Diffusion of gaseous products through the gas film back into the main body of fluid.

Diffusion through Gas Film Controls

In this regime the resistance of the gas film controls, indicates that no gaseous reactant is present at the particle surface and the concentration driving force, $C_{Ag} - C_{As}$ becomes C_{Ag} and is constant at all times during reaction of the particle. Hence, the time for complete conversion of a particle will be:

$$\mathcal{T} = \frac{\rho_B R}{3bk_{Ag}C_{Ag}} \quad (1)$$

And the conversion X_A is defined as:

$$t/\mathcal{T} = X_A \quad (2)$$

The carbonation reaction is:



With the assumption of ideal gas phase, where

$$PV = nRT \quad (5)$$

Film resistance at the surface of a particle is dependent on numerous factors, such as the relative velocity between particle and fluid, size of particle, and fluid properties. These factors have been correlated for various ways of contacting fluid with solid, such as packed beds, fluidized beds. Froessling (1938) gave, an example, for mass transfer of a component of mole fraction (y) in a fluid to free-falling solid. Theoretical maximum weight gain (%) of CaO = 78 mg of CO₂/mg of CaO and theoretical maximum weight gain % of NaOH = 37 mg of CO₂/100 mg of NaOH:

$$\text{Sh} = 2 + 0.6(\text{Sc})^{1/3}(\text{Re})^{1/2} \quad (6)$$

$$\frac{k_{Ag} h d_p y}{\mathcal{D}} = 2 + 0.6(\text{Sc})^{1/3}(\text{Re})^{1/2} = 2 + 0.6 \left(\frac{\mu}{\rho \mathcal{D}} \right)^{1/3} \left(\frac{dp u \rho}{\mu} \right)^{1/2} \quad (7)$$

In order to estimate time required for complete conversion in a gas film controls regime, the following procedure has been used: Chapman

and Enskog equation (Poling *et al*, 2001) for describing self diffusivity coefficient for gas (self diffusion of CO₂):

$$\mathcal{D}_{(\text{CO}_2\text{-CO}_2)} = (0.00266T^{3/2}) / (PM^{1/2}\sigma^2\Omega_D) \quad (8)$$

$$\sigma_{AA} = (\sigma_A + \sigma_A) / 2 \quad (9)$$

$$\Omega_D = A / (T^*)^B + C / \exp(DT^*) + E / \exp(FT^*) + G / \exp(HT^*) \quad (10)$$

$$(\mathcal{D}_{T1} / \mathcal{D}_{T2}) = (T_1 / T_2)^{3/2} \quad (11)$$

Where:

$$T^* = kT / \varepsilon_{AA}, A = 1.06036, B = 0.15610, C = 0.19300, D = 0.47635, E = 1.03587, F = 1.52996, G = 1.76474, H = 3.89411, \sigma_{\text{CO}_2} = 3.941 \text{ \AA}, \varepsilon_{(\text{CO}_2)/k} = 195.2\text{K}, \text{ and } \Omega_D = 0.87486.$$

Diffusion through Ash Layer Controls

In this regime the resistance to diffusion through the ash controls the rate of reaction so that both reactant (A) and the boundary of the unreacted core move inward toward the center of the particle. Where the time (T) required for complete conversion is:

$$T = \frac{\rho_B R^2}{6b\mathcal{D}_e C_{Ag}} \quad (12)$$

$$t/T = 1 - 3(1 - X_A)^{2/3} + 2(1 - X_A) \quad (13)$$

Chemical Reaction Controls

The progress of the reaction is unaffected by the presence of any ash layer, the rate is proportional to the available surface of unreacted core. Where the time (T) required for complete conversion is

$$T = \frac{\rho_B R}{bk'' C_{Ag}} \quad (14)$$

$$t/T = 1 - (1 - X_A)^{1/3} \quad (15)$$

RESULTS AND DISCUSSION

Carbonation of Calcium Oxide

The reaction of CO₂-CaO proceeds through two rate-controlling regimes. The first regime involves a rapid, heterogeneous chemical reaction. In the second regime, the reaction slows down due to the formation of an impervious layer of CaCO₃. This product layer prevents the exposure of unreacted CaO in the particle core to CO₂ for further carbonation. The kinetics of the second regime is governed by the diffusion of gaseous species

through the CaCO₃ product layer. However, the relative importance of the gas film, ash layer, and reaction steps will vary as particle conversion progresses. For example, for a constant size particle the gas film resistance remains unchanged, the resistance to reaction increase as the surface of unreacted core decreased, while the ash layer resistance was nonexistent at the start because no ash is present, but became progressively more and more crucial as the product layers build up.

Scanning electron microscope (SEM) images for pure CaO, CaO and CO₂ reactant samples at various temperatures have shown in (Fig. 2). Figure 3 represents the film diffusion controls, ash diffusion controls and reaction controls for CO₂-CaO system which changes with time and affected significantly by high temperature ranges (> 550°C). Table 1 gives the molecular diffusion coefficient (\mathcal{D}) from Chapman and Enskog equation (8), mass transfer coefficient (k_{Ag}) which has been calculated from Froessling equation (7), and the time for complete conversion of a CaO particle with gas film controls ($\mathcal{T}_{\text{film}}$) using equation (1). Time required to complete conversion for gas film control regime within the temperature range from 550°C to 750°C indicated that this control regime is not rate limiting mechanism. The time required for achieving high conversions exceeding times longer than 50 seconds as shown in (Figs. 4-8).

The initial linear stage identifies the kinetic control regime with the slope of this stage giving the intrinsic surface reaction rate. Furthermore, the starting points of the linear stage, featuring the maximum slope, usually reside at low conversions, i.e. 5% to 7%. As carbonation proceeds product layer diffusion becomes more crucial, resulting in much slower carbonation rate. The shrinking core model which has been applied for CO₂-CaO system when chemical kinetics control the overall reaction (Equations 13 & 14) that is also equivalent to grain model that has been described by Szekely *et al* (1976).

Table 2 illustrates the effect of temperature on chemical reaction rate constant (k'') between gas (CO₂) and particles (CaO) calculated from equation (14). Even though there is scattered in surface reaction rate constants given in Table 2 which could be due to non uniform solid sample and its transformation as a result of thermal stresses, causing surface area to vary as a function of temperature. Activation energy obtained from this data gave of 12kJ/mole as shown in (Fig. 9).

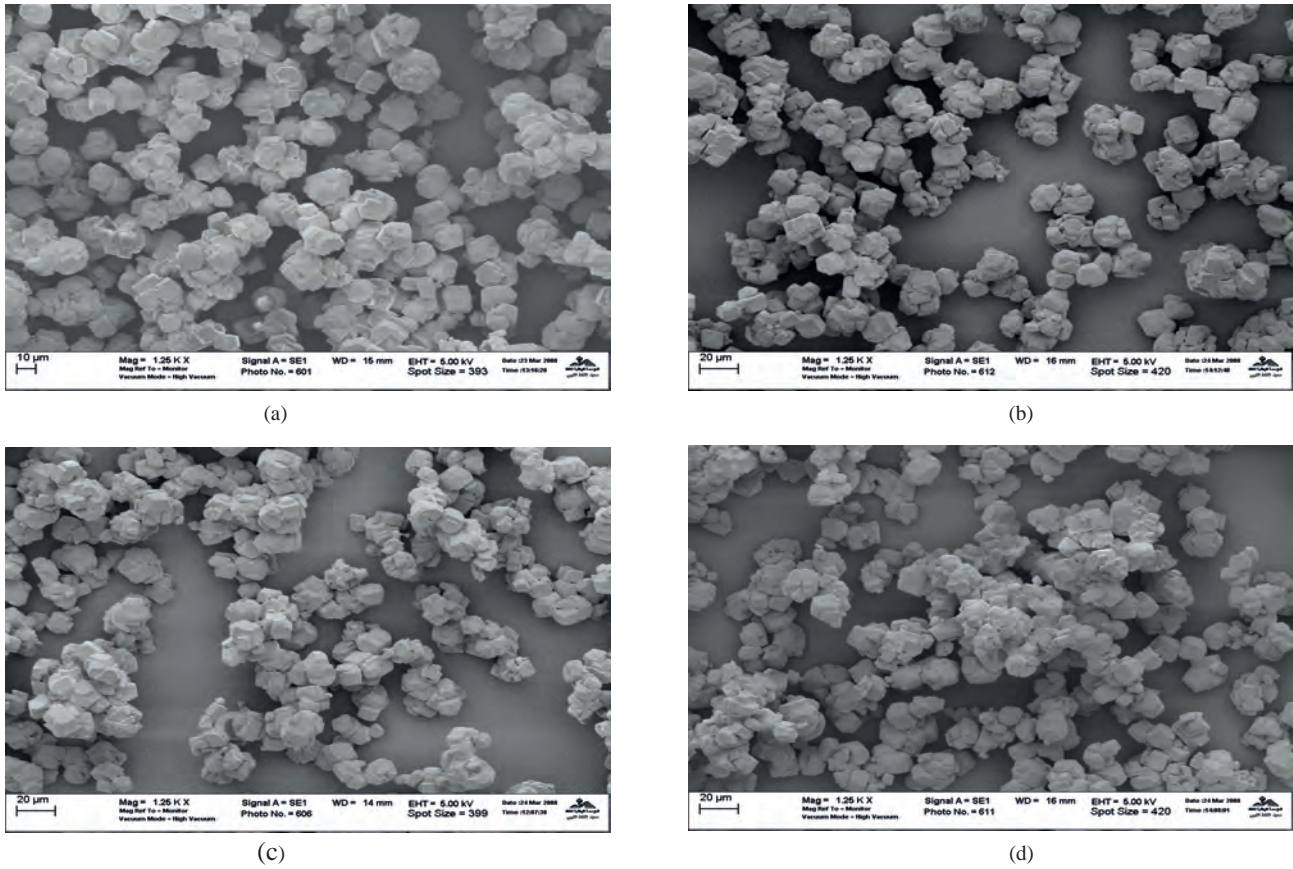


Fig. 2. SEM images (1250X) of pure calcium carbonate (CaCO₃) (a), calcined calcium carbonate (CaCO₃) at 1000°C (b), CaO-CO₂ reaction sample at 550°C (c) and CaO-CO₂ reaction sample at 700°C (d)

Table 1. Estimated molecular diffusion coefficient (\mathcal{D}), mass transfer coefficient (k_{Ag}) and time for complete conversion (T_{film}) assuming gas film regime controls for the CaO-CO₂ system

Temperature (°C)	ρ_{CO_2} (kg/m ³)	μ_{CO_2} (kg/sec*m)	$C_{Ag(CO_2)}$ (mol/m ³)	\mathcal{D} (m ² /sec)	k_{Ag} (m/sec)	T_{film} (sec)
550	0.6516	0.3962	14.8	0.00006969	2.8616	0.01151
600	0.6143	0.4131	13.95	0.000076135	3.1254	0.01118
650	0.581	0.4296	13.2	0.000082767	3.3968	0.010875
700	0.5511	0.4460	12.5	0.000089582	3.6757	0.010613
750	0.5242	0.4623	11.91	0.000096574	3.9618	0.010334

This activation energy is lower than values which have been reported by Sun *et al* (2008a & b) which found activation energy of 29 ± 4 kJ/mole for CaO obtained from natural limestone which indicates that this reaction is faster than that reported by Sun *et al* (2008a & b). However, Sun *et al* (2008a & b) who studied the kinetics of this system (CO₂-CaO) using various models suggested activation energies near zero, which is an average value between present activation energy and those reported in (Sun *et al* 2008a & b). The effective diffusion coefficient (\mathcal{D}_e) of gaseous reactant in the ash layer calculated from equation (12) and the

time (T) required for complete conversion in both chemical reaction and ash diffusion regimes from (Figs. 4-8). Times for complete conversion for ash diffusion controls regime within the temperature ranges of 550°C to 750°C as shown in Table 2 indicating that this control regime is the major rate controlling step. Effective diffusion coefficients reported in the Table 2 are much smaller than molecular diffusion coefficients given in (Table 2) indicating that either Knudsen and/or surface diffusion mechanisms are operating within the pores of calcium carbonate. Actually, effective diffusion coefficients are of combined Knudsen/

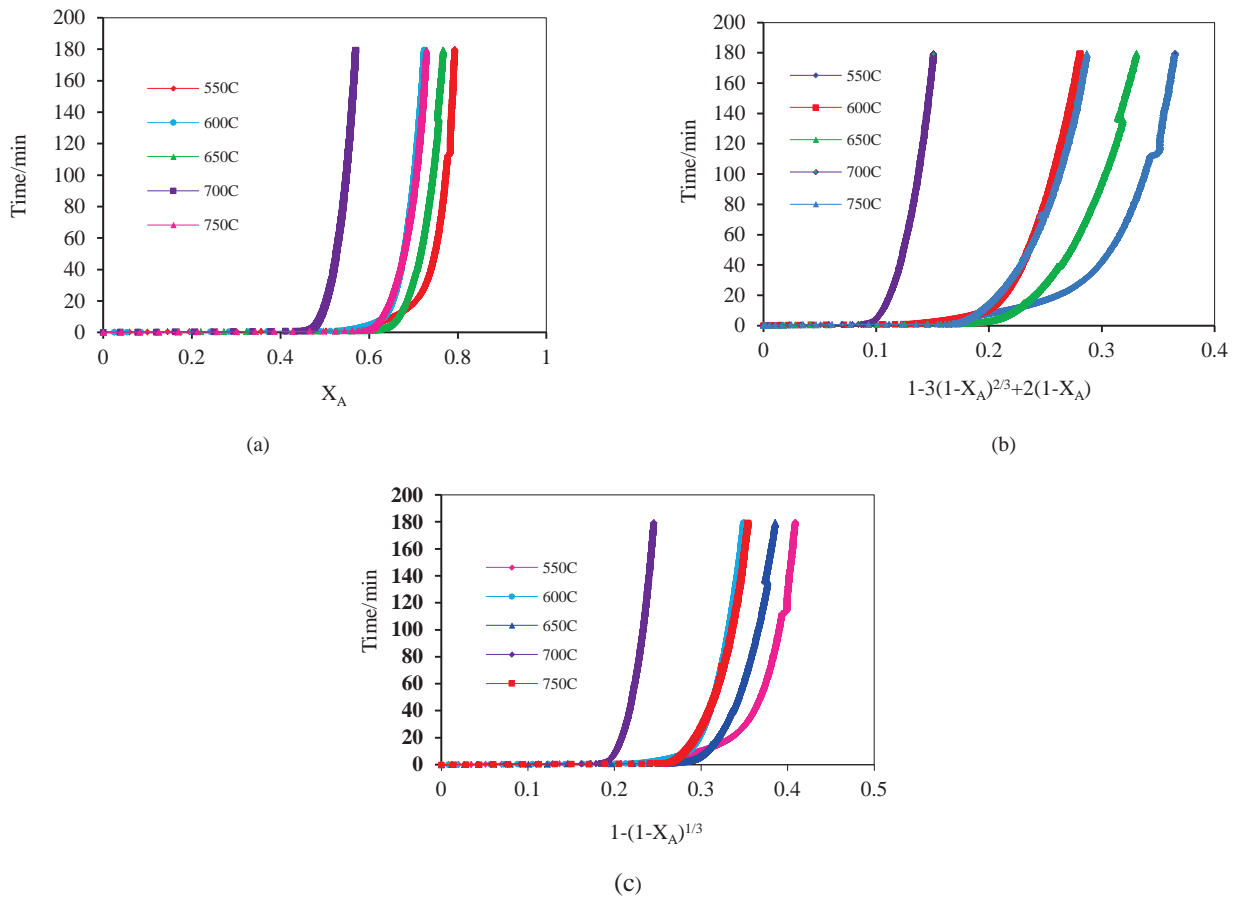


Fig. 3. Conversion vs time for (a) gas film controls, (b) chemical reaction controls and (c) ash diffusion controls carbonatation cycle for CO₂-CaO system

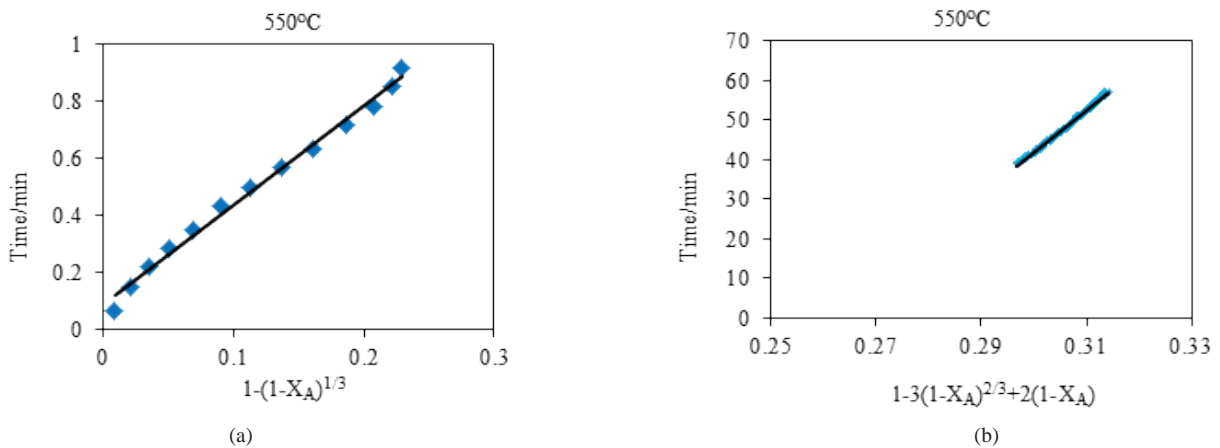


Fig. 4. Slope of reaction of CaO-CO₂ with the aid of Shrinking Core model during early stage (a) of carbonation and diffusion product layer of CaO-CO₂ during final stage (b) of calcium oxide at 550°C

Surface diffusion types because their values are of the order of 10^{-12} m²/sec but with restricted activation giving activation energy in the order of 20kJ/mol. Knudsen diffusion has temperature dependency of 0.5 whereas, surface diffusion usually shows a temperature variation of greater

than 15. Present data temperature dependency is of the order of 3. Shrinking unreacted core model without structural variation has a limitation in completely describing quantitatively in this reaction system. Shrinking core model gave reasonable representation and at rest semi-quantitative for

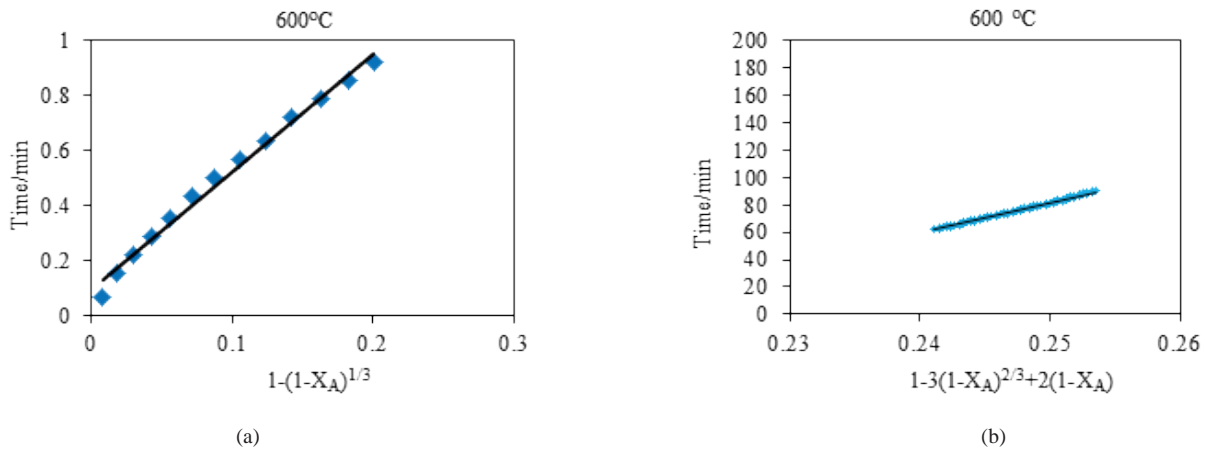


Fig. 5. Slope of reaction of CaO-CO₂ with the aid of Shrinking Core model during early stage (a) of carbonation and diffusion product layer of CaO-CO₂ during final stage (b) of calcium oxide at 600°C

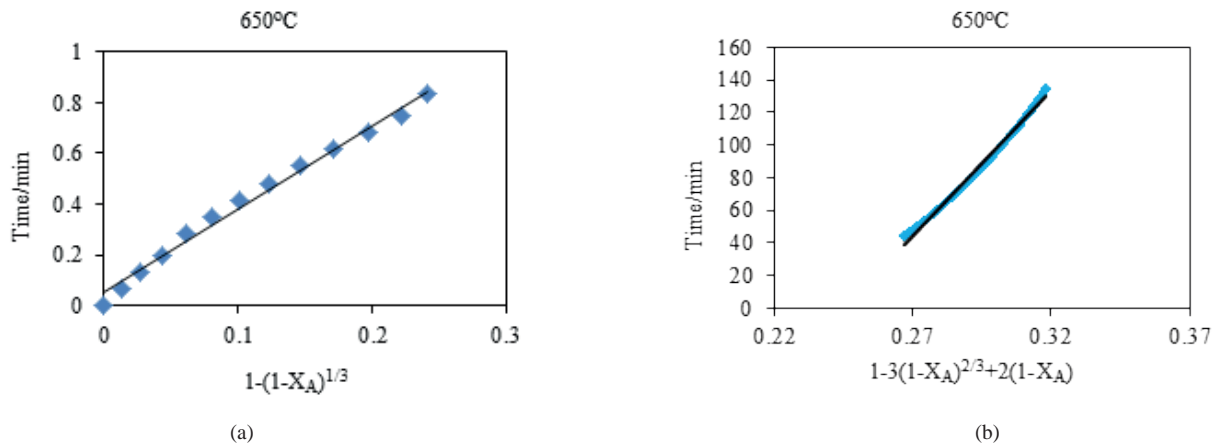


Fig. 6. Slope of reaction of CaO-CO₂ with the aid of Shrinking Core model during early stage (a) of carbonation and diffusion product layer of CaO-CO₂ during final stage (b) of calcium oxide at 650 °C

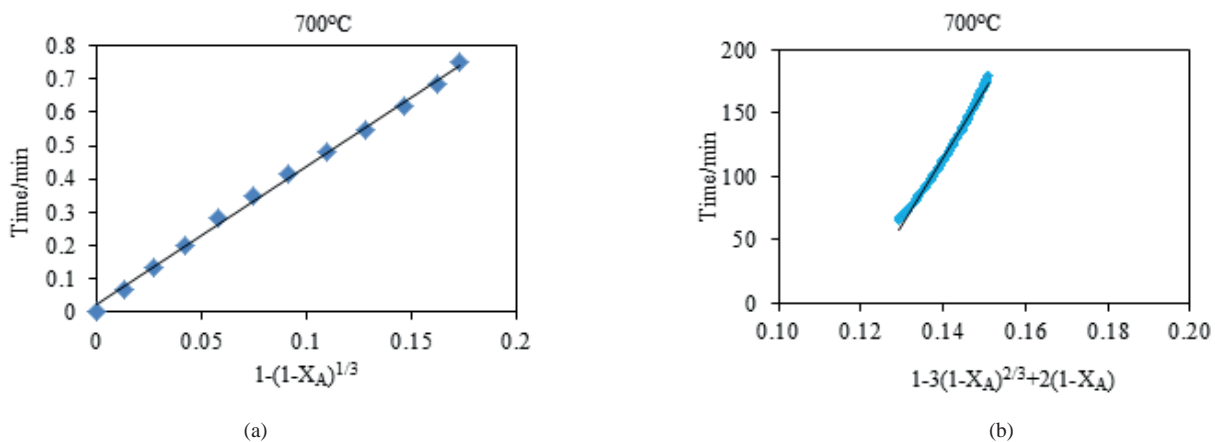


Fig. 7. Slope of reaction of CaO-CO₂ with the aid of Shrinking Core model during early stage (a) of carbonation and diffusion product layer of CaO-CO₂ during final stage (b) of calcium oxide at 700°C

CO₂-CaO reaction system. Modeling approach employing a variable diffusivity shrinking core model (Szekely *et al*, 1976) or a variable pore size distribution model (Levenspiel *et al*, 1999) would provide a better gas–solid reaction model.

After times exceeding roughly 50 seconds, rate of reaction slows down due to the resistance to diffusion generated from the formation of CaCO₃ layer (ash) as described above. The shrinking core model under ash diffusion controls has short

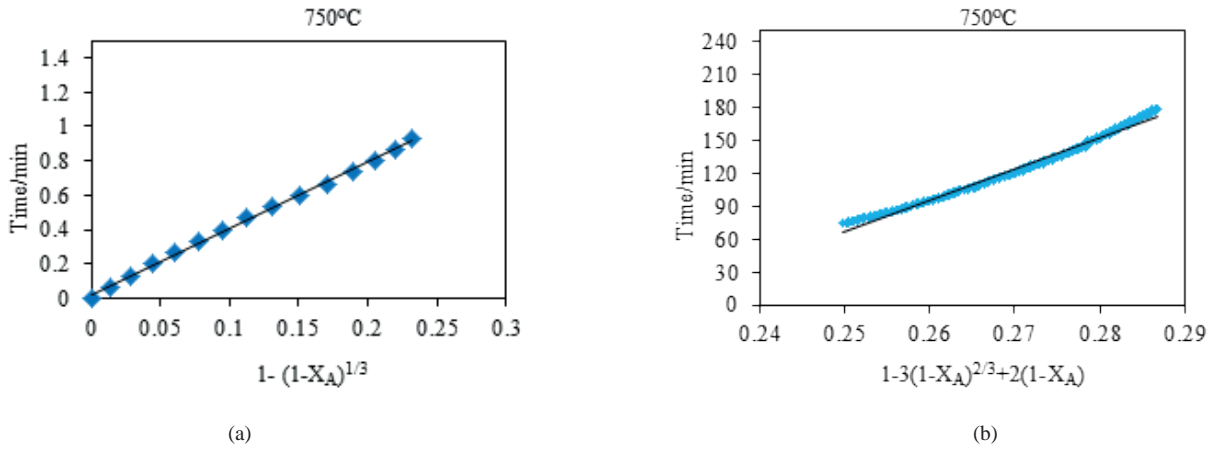


Fig. 8. Slope of reaction of CaO-CO₂ with the aid of Shrinking Core model during early stage (a) of carbonation and diffusion product layer of CaO-CO₂ during final stage (b) of calcium oxide at 750°C

Table 2. Chemical reaction rate constant (k^*) between gas (CO₂) and particles (CaO) and effective diffusion coefficient (\mathcal{D}_e) of gaseous reactant in the ash layer and the time (τ_{reaction}) & ($\tau_{\text{diffusion}}$) required for complete conversion for both chemical reaction and ash diffusion regimes

Temperature/°C	$\tau_{\text{diffusion}}/\text{sec}$	$\mathcal{D}_e(\text{m}^2/\text{sec})$	$\tau_{\text{reaction}}/\text{sec}$	$k^*(\text{m}/\text{sec})$
550	137520	2.93418E-12	209.43	0.00047184
600	134460	3.18324E-12	256.2	0.00040914
650	106620	4.24431E-12	197.94	0.00055988
700	314880	1.51498E-12	250.08	0.00046715
750	171720	2.92073E-12	231.48	0.00053062

coming in totally describing this behavior as shown in (Figs. 4 to 8). According to equation (13) plots must pass the origin so, estimated diffusion coefficients are only approximate values, because it is suspected that CaCO₃ solid layer is not completely impervious or nonporous for which shrinking core model with diffusion control has been originally proposed. This data could be empirically modified to estimate the time for complete conversion of a particle at ash diffusion controls regime using a power and exponential relations:

$$t = (a_o)e^{a_1} (X_A) \quad (16)$$

$$t = b_o (X_A)^{b_1} \quad (17)$$

Figure 10 presents the fit of the experimental data with exponential and power correlations for ash diffusion controls regime and (Table 3) gives the parameters of those correlations which

indicated that the CO₂-CaO system data can be fitted with exponential and power correlations.

Carbonation of Caustic Soda

Scanning electron microscope (SEM) images for pure NaOH, CO₂ and NaOH reactant samples at various temperatures have shown in (Fig. 11). The film diffusion controls, the ash diffusion controls and chemical reaction controls for CO₂-NaOH system which changed with the time and affected by various temperature ranges have been shown in (Fig. 12). Table 4 gives the molecular diffusion coefficient (\mathcal{D}) from Chapman and Enskog equation (8), mass transfer coefficient (kAg) which has been calculated from Froessling equation (7), and the time for complete conversion of a particle within the gas film (T_{film}) using equation (1). Time for complete conversion for gas film controls regime within temperature range 75°C to 225°C around 11 sec indicating that this control regime is not rate limiting

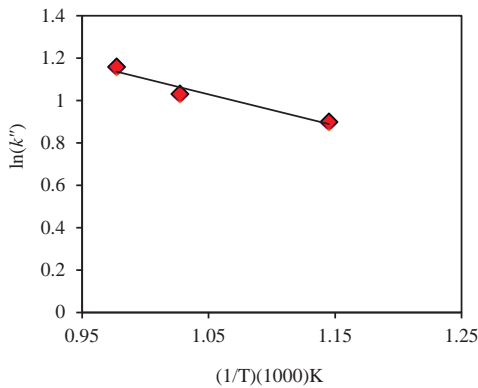
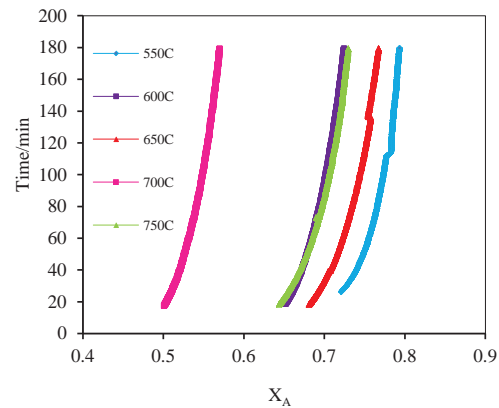

 Fig. 9. Arrhenius plot for chemical reaction rate constant (k'') at high temperature range

 Fig. 10. Correlating high conversion range with empirical power and exponential equations for CaO-CO₂ reaction system

 Table 3. Empirical power and exponential equations for fitting high conversion range with power and exponential equations for CaO-CO₂ reaction system

Temperature/°C	Exponential Equation: $t = (a_0)e^{a_1(X_A)}$			Power Equation: $t = b_0(X_A)^{b_1}$		
	a_0	a_1	R^2	b_0	b_1	R^2
550°C	9E-08	26.87	0.995	19232	20.49	0.994
600°C	8E-08	29.81	0.994	14375	20.58	0.996
650°C	6E-07	25.48	0.997	25020	18.63	0.998
700°C	3E-06	31.71	0.992	3E+06	17.11	0.995
750°C	2E-06	25.28	0.998	43810	17.49	0.999

mechanism compared with experimental time for achieving more than 60% conversion exceeding 3600sec as shown in (Fig. 12). This clearly indicates that gas film controls is not dominant control mechanism. Gas film resistance may only influence the reaction during few seconds at the beginning, where the reaction rate is fast within the period which commonly known as the starvation period. The kinetic control regime and ash diffusion controls regime were based on the shrinking core model as shown in (Figs. 13-19) and calculated from equations (12 & 13) and (14 & 15). The initial linear stage identifies the kinetic control region with the slope of this stage giving the intrinsic surface reaction rate. The starting points of the linear stage, featuring the maximum slope, usually reside at low conversions, i.e. 6%. As carbonation proceeds further, product-layer diffusion became more significant, resulting in much slower carbonation rate due to the formation of sodium carbonate. This has been

clearly seen from SEM micrographs given in (Fig. 11) which provide the effect of temperature on chemical reaction rate constant (k'') between fluid (CO₂) and NaOH particles and the effective diffusion coefficient ($\mathcal{D}e$) of gaseous reactant in the ash layer (Na₂CO₃ layer) as shown in (Table 5). Activation energy obtained from (k'') data is estimated to be 13kJ/mol and the results are shown in (Fig. 20). Time for complete conversion for ash diffusion controls regime within temperature range of 75°C to 225°C indicates that the ash diffusion control regime is the major rate controlling step compared with experimental time for achieving high conversion 27mg of CO₂ per 100mg of NaOH after 2760sec at 225°C. The effective diffusion coefficients which reported in Table 5 are much smaller than the molecular diffusion gas coefficients as shown in (Table 4). This could be due to the formation of Na₂CO₃ with a low diffusion coefficient into its structure. According to the equation (13) plots must pass

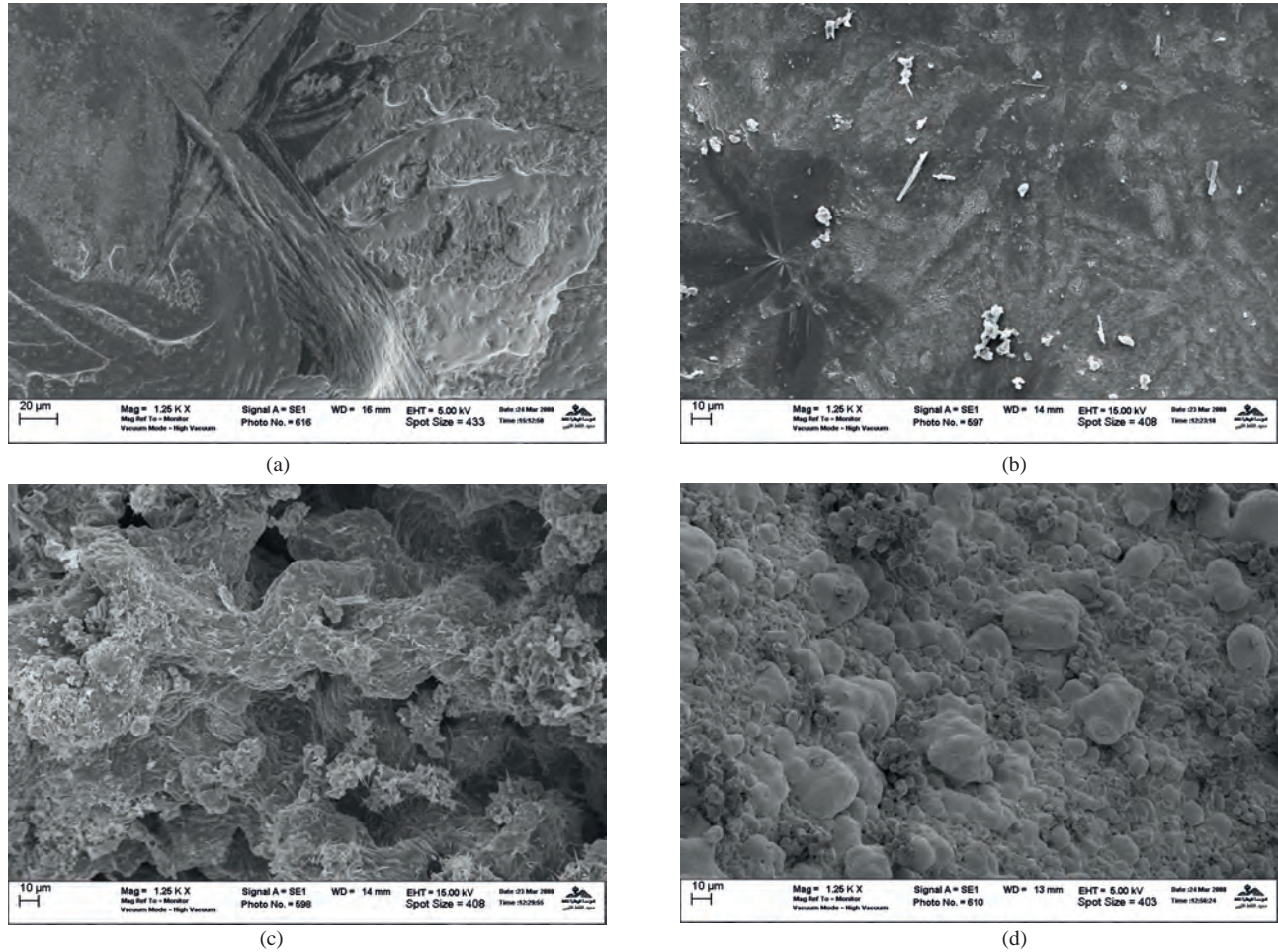


Fig. 11. SEM image (1250X) of calcined caustic soda (NaOH) sample (a), NaOH-CO₂ reaction sample at 150°C (b) NaOH-CO₂ reaction sample at 200°C (c) and NaOH-CO₂ reaction sample at 225°C (d)

the origin so, estimated diffusion coefficients are only approximate values as shown in (Fig. 21). Empirical equations (16) and (17) could be used to estimate the time for complete conversion of a particle for ash diffusion controls regime as shown in (Table 6).

CONCLUSIONS

The shrinking unreacted core model for gas solid non-catalytic reactions has been utilized to describe CO₂-CaO and CO₂-NaOH reaction systems. This model has been found to semi quantitatively in describing these reactions. In CaO and NaOH systems, gas film resistance has been ruled out as rate controlling step since complete conversion times were much smaller (0.015 and 12 seconds) than actual times (137 minutes for CaO and 60 minutes for NaOH)

required to achieve high conversions above 70% for CaO and above 60% for NaOH. Reaction rate was established as rate controlling step for both CaO and NaOH systems within earlier times. Activation energies were estimated about 12 kJ/mol and 13 kJ/mol respectively. These energies have been found to agree with those obtained from initial rates analysis. CO₂-CaO and CO₂-NaOH reactions after initial times were larger than 1.5 minutes. Reactions become dominated by diffusion of CO₂ reactant with CaCO₃ and Na₂CO₃ solid product layers. Estimated effective diffusion coefficients of the order of 10⁻¹² and 10⁻¹⁰ m²/sec for CaO and NaOH systems respectively were below those for molecular diffusion with values of the order of 10⁻⁴ and 3 x 10⁻⁵ m²/sec for the same systems. These effective diffusion coefficients are within diffusion transport *via* Knudsen and/or surface flows.

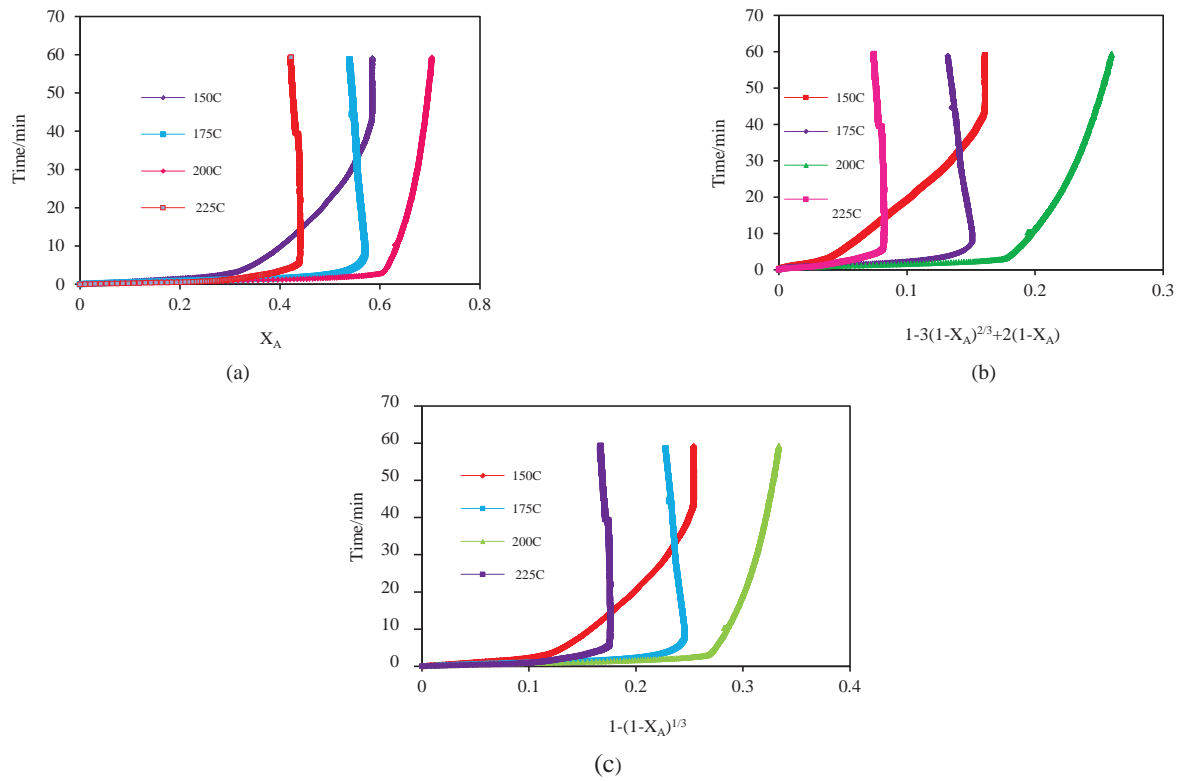


Fig. 12. Conversion vs time for (a) gas film controls, (b) chemical reaction controls and (c) ash diffusion controls at the carbonation cycle for CO₂-NaOH system

Table 4. Estimated molecular diffusion coefficient (\mathcal{D}), mass transfer coefficient (k_{Ag}) and time for complete conversion (\mathcal{T}_{film}) assuming gas film regime controls for the NaOH-CO₂ system

Temperature (°C)	ρ_{CO_2} (kg/m ³)	μ_{CO_2} (kg/sec.m)	$C_{Ag(CO_2)}$ (mol/m ³)	\mathcal{D} (m ² /sec)	k_{Ag} (m/sec)	\mathcal{T}_{film} (sec)
75	1.546	0.1738	0.00350	0.000019169	0.0206706	12.0967
100	1.442	0.1879	0.00326	0.000021272	0.022844	11.7523
125	1.35	0.2020	0.00306	0.000023358	0.0249920	11.444
150	1.27	0.2162	0.00288	0.000025592	0.0272917	11.135
175	1.199	0.2303	0.00272	0.0000278937	0.0293837	10.9506
200	1.135	0.2443	0.002575	0.000030260	0.0320834	10.5939
225	1.078	0.2581	0.002446	0.0000326897	0.0345801	10.3474

Table 5. Chemical reaction rate constant (k^*) between gas (CO₂) and particles (NaOH) and effective diffusion coefficient (\mathcal{D}_e) of gaseous reactant in the ash layer and the time ($\mathcal{T}_{reaction}$) & ($\mathcal{T}_{diffusion}$) required for complete conversion for both chemical reaction and ash diffusion regimes

Temperature/°C	$\mathcal{T}_{diffusion}/sec$	$\mathcal{D}_e(m^2/sec)$	$\mathcal{T}_{reaction}/sec$	$k^*(m/sec)$
75	22066.4	6.05E-08	1200.6	0.000928
100	41442	3.23E-09	482.16	0.002476
125	3176.4	4.50E-08	653.4	0.001949
150	36504	4.16E-09	1245.6	0.001087
175	20406	7.88E-09	568.44	0.002522
200	58200	2.92E-09	425.58	0.003557
225	351840	5.08E-10	452.28	0.003524

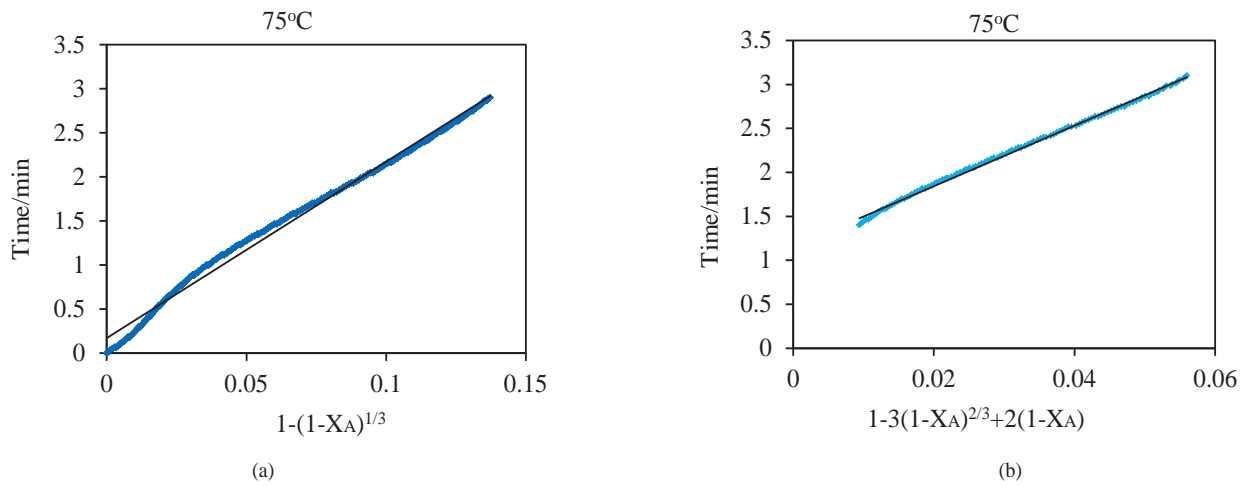


Fig. 13. Slopes of reaction of NaOH-CO₂ with the aid of the Shrinking Core model at 75°C during early stage (a) and diffusion product layer of NaOH-CO₂ with the aid of the model during final stage (b) of carbonation for NaOH.

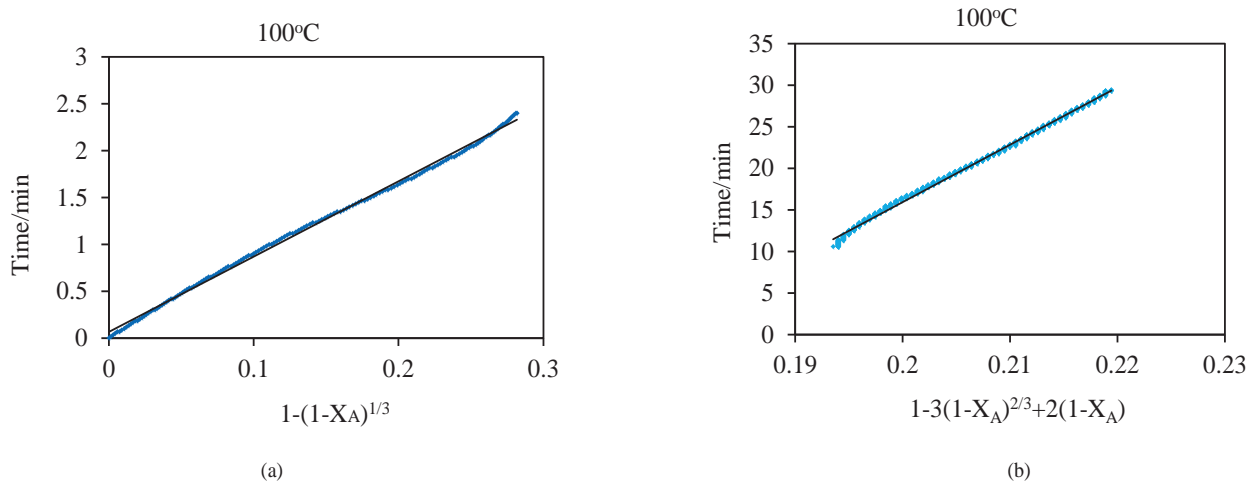


Fig. 14. Slopes of reaction of NaOH-CO₂ with the aid of the Shrinking Core model at 100°C during early stage (a) and diffusion product layer of NaOH-CO₂ with the aid of the model during final stage (b) of carbonation for NaOH.

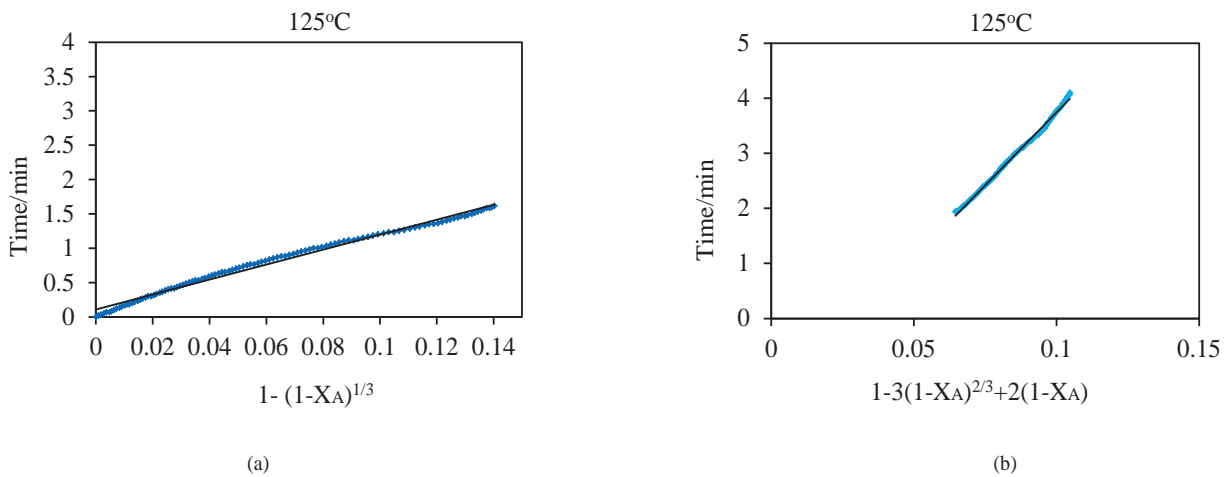


Fig. 15. Slopes of reaction of NaOH-CO₂ with the aid of the Shrinking Core model at 125°C during early stage (a) and diffusion product layer of NaOH-CO₂ with the aid of the model during final stage (b) of carbonation for NaOH.

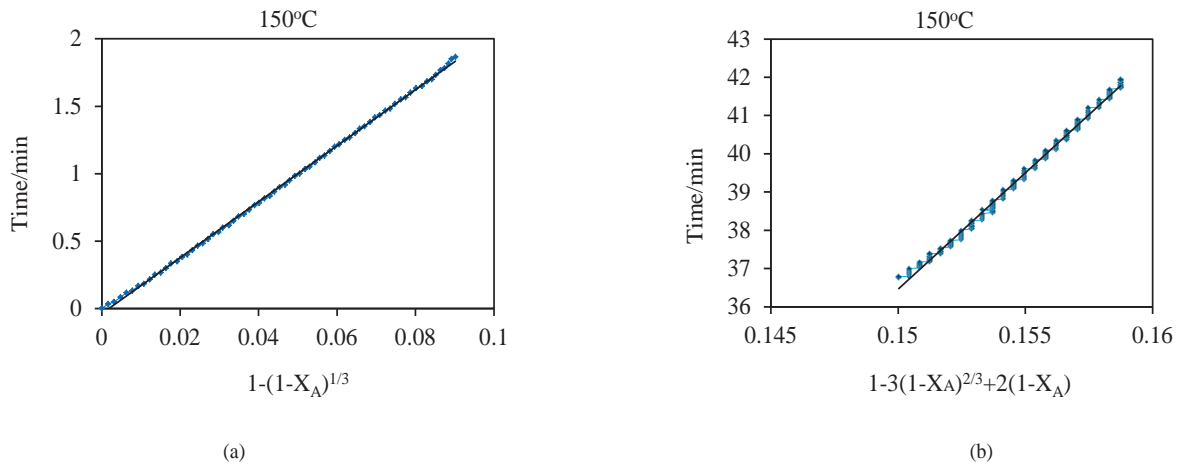


Fig. 16. Slopes of reaction of NaOH-CO₂ with the aid of the Shrinking Core model at 150°C during early stage (a) and diffusion product layer of NaOH-CO₂ with the aid of the model during final stage (b) of carbonation for NaOH.

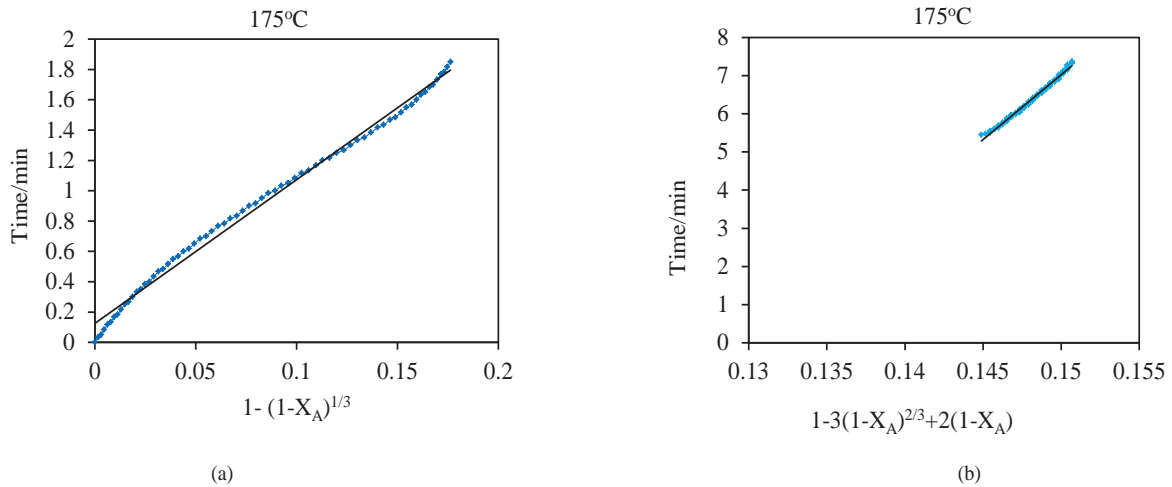


Fig. 17. Slopes of reaction of NaOH-CO₂ with the aid of the Shrinking Core model during early stage (a) and diffusion product layer of NaOH-CO₂ with the aid of the model during final stage (b) of carbonation for NaOH at 175°C

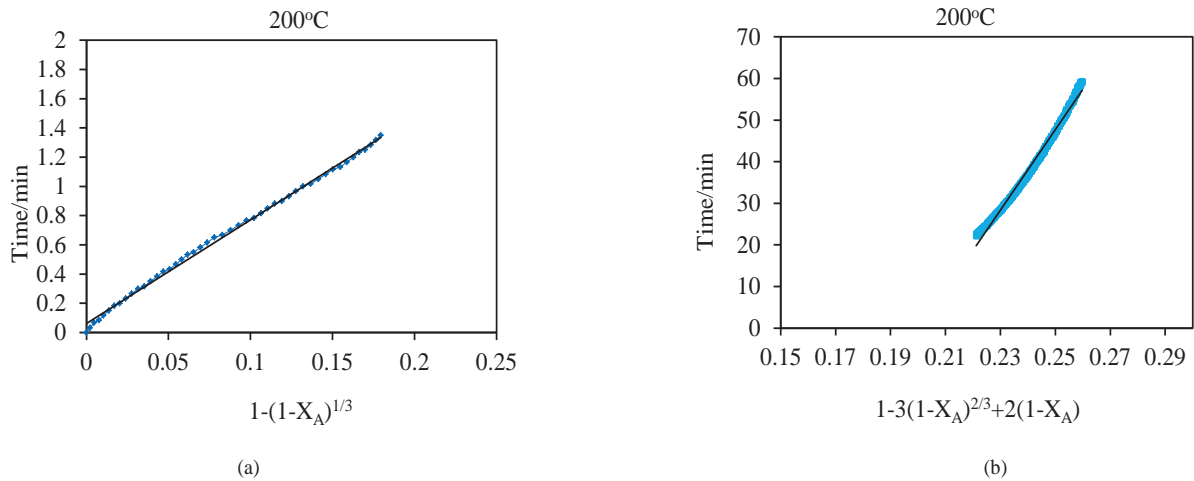


Fig. 18. Slopes of reaction of NaOH-CO₂ with the aid of the Shrinking Core model during early stage (a) and diffusion product layer of NaOH-CO₂ with the aid of the model during final stage (b) of carbonation for NaOH at 200°C

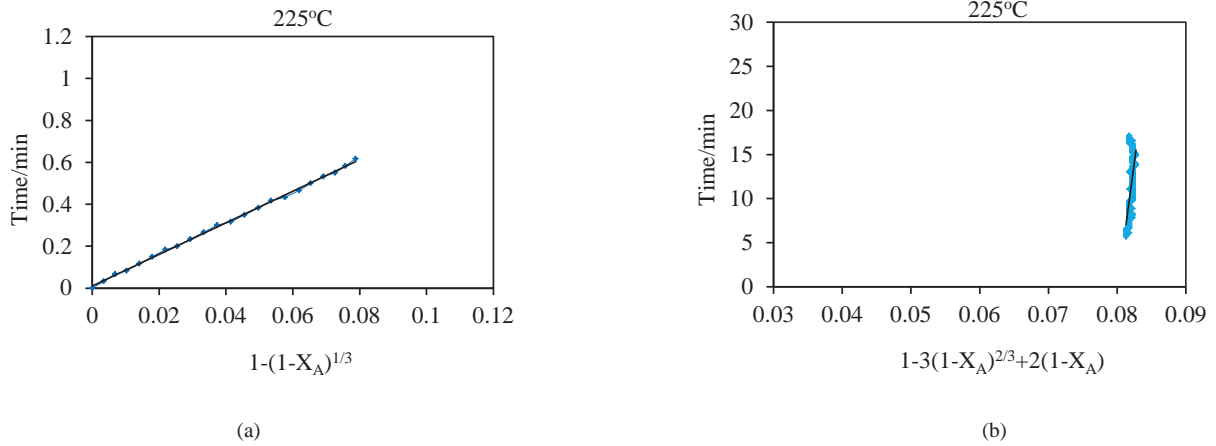


Fig. 19. Slopes of reaction of NaOH-CO₂ with the aid of the Shrinking Core model at 225°C during early stage (a) and diffusion product layer of NaOH-CO₂ with the aid of the model during final stage (b) of carbonation for NaOH.

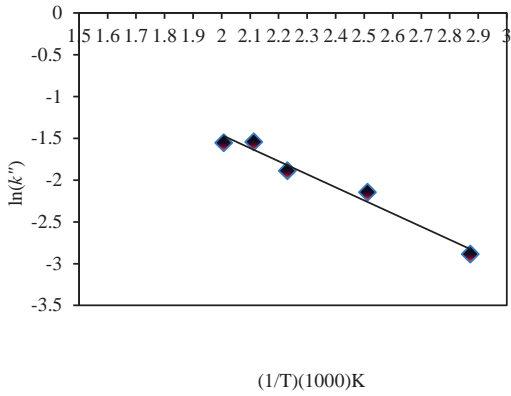


Fig. 20. Arrhenius plot for chemical reaction rate constant (k') at low temperature range

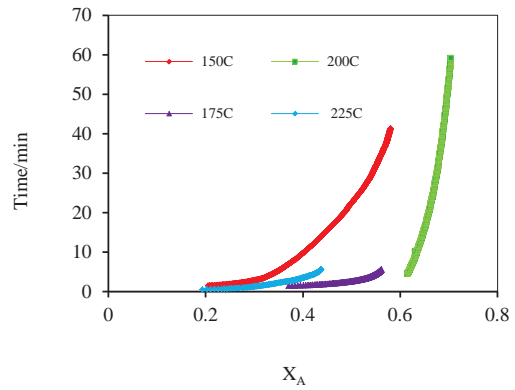


Fig. 21. Correlating high conversion range with empirical power and exponential equations for NaOH-CO₂ reaction system

Table 6. Empirical power and exponential equations for fitting high conversion range with power and exponential equations for NaOH-CO₂ reaction system

Temperature/°C	Exponential Equation: $t = (a_0)e^{a_1(X_A)}$			Power Equation: $t = b_0(X_A)^{b_1}$		
	a_0	a_1	R^2	b_0	b_1	R^2
150 °C	0.249	8.9	0.985	313.1	3.811	0.993
175 °C	0.061	7.689	0.93	37	3.642	0.902
200 °C	6E-07	26.22	0.992	27796	17.43	0.994
225 °C	0.062	10	0.996	75.5	3.332	0.620

NOMENCLATURE

- X_A (weight gain % mg of CO₂/mg sorbent)/(theoretical maximum weight gain % of sorbent)
- T Time for complete conversion a particle (CaO & NaOH) (sec) at gas film controls
- t Time experiment for the reaction of CO₂ with solid sorbents (CaO/NaOH) (sec)
- ρ_B Molar density of solid sorbents ($\rho_{CaO} = 0.05971 \text{ mol/cm}^3$ & $\rho_{NaOH} = 0.052513 \text{ mol/cm}^3$)
- b Stoichiometry coefficient of solid sorbents (1 for CaO & 2 for NaOH)
- k_{Ag} Mass transfer coefficient between fluid (CO₂) and particle (CaO/NaOH) (m/min)
- C_{Ag} Concentration of gaseous reactant (CO₂) (mol/cm³)
- P Atmospheric pressure (1atm)

R	Ideal gas constant (82.056 cm ³ atm/mol K)
T	Temperature (K)
Sc	Schmidt number
Re	Reynolds number
Sh	Sherwood number
k_{Ag}	Mass transfer coefficient between fluid (CO ₂) and particles (CaO/NaOH) (m/sec)
d_p	Diameter of solid sorbent particles (0.0049cm for CaO & 0.2 cm for NaOH)
y	Mole fraction of the fluid (CO ₂)
\mathcal{D}	Molecular diffusion coefficient (m ² /sec)
μ	Kinematic viscosity of fluid (CO ₂) (cp)
ρ	Mass density of the fluid (CO ₂)
u	Gas (CO ₂) velocity = 1.179cm/sec
$\mathcal{D}_{(CO_2)}$	Self-diffusion coefficient (m ² /sec)
σ_{AA}	Characteristic length (Å)
Ω_D	Diffusion collision integral, dimensionless
M_{CO_2}	44 g/mol
R	Diameter of solid sorbents particles (R_{CaO} =0.00245cm & R_{NaOH} =0.1cm)
\mathcal{D}_e	Effective diffusion coefficient (m ² /sec)
k''	Chemical reaction rate constant (m/sec)

REFERENCES

- Abanades, J. C. and Alvarez, D. (2003). Conversion Limits in the Reaction of CO₂ with Lime. *Energy and Fuels*, **17**: 308-315.
- Abunowara, M.; Bustam, M. A.; Sufian, S.; Babar, M.; Eldemerdash, U.; Suleman, H.; Bencini, R. and Ullah, S. (2020). Experimental Measurements of Carbon Dioxide, Methane and Nitrogen High-Pressure Adsorption Properties onto Malaysian Coals under Various Conditions. *Energy* **210**: 118575.
- Alvarez, D. and Abanades, J. C. (2005). Determination of the Critical Product Layer Thickness in the Reaction of CaO with CO₂. *Industrial & Engineering Chemistry Research*, **44**: 5608-5615.
- Aydin, G.; Karakurt, I. and Aydiner, K. (2010) Evaluation of Geologic Storage Options of CO₂: Applicability, Cost, Storage Capacity and Safety. *Energy Policy*, **V**, **38**: 5072-5080.
- Barker, R. (1973). The Reversibility of the Reaction CaCO₃ = CaO + CO₂. *Jour. App. Chem. Biotech.*, **23**: 733-742.
- Bhatia, S. K. and Perlmutter, D. D. (1983). Effect of the Product Layer on Kinetics of the CO₂ Lime Reaction. *A. I. Ch. E. Jour.*, **29**: 79-86.
- Bhattacharya, A. and Purohit, P. (2004). Predicting Reaction Rates for Non-Catalytic Fluid-Solid Reactions in Presence of Structural Changes in the Solid Phase. *Chem. Eng. J.*, **102**: 141-149.
- Breidenich, C.; Magraw, D.; Rowley, A. and Rubin, J. W. (1998). The Kyoto Protocol to the United Nations Framework Convention on Climate Change. *The American Journal of International Law*, **V**, **92**: 315-331.
- Froessling, N. (1938). Über die verdunstung fallender tropfen. *Gerland Beitr Geophys*, **52**: 170p.
- Hu, Y.; Lu, H. and Li, H. (2021). Li₄SiO₄ Pellets Templated by Rice husk for Cyclic CO₂ Capture: Insight into the Modification Mechanism. *Ceramics International* **47.22**: 32060-32067.
- Huaman R. N. E. and Jun, T. X. (2014). Energy Related CO₂ Emissions and the Progress on CCS Projects: A Review. *Renewable and Sustainable Energy Reviews*, **V**, **31**: 368-385.
- Levenspiel, O. (1999). Chemical Reaction Engineering. **3rd**: 704.
- Lin, J.; Lu, W.; Shi, X.; Lu, Q.; Wang, L. and He. H. (2021). Design of an Intelligent Nanofiber-Based Solid Amine Adsorbent with High CO₂ Capture Capacity and an Ultralow Regeneration Temperature. *ACS Sustainable Chem. Eng.*, **9**: 10184-10195.
- Pachauri, R. K.; Allen, M. R.; Barros, V. R.; Broome, J.; Cramer, W.; Christ, R.; Church, J. A.; Clarke, L.; Dahe, Q.; Dasgupta, P. (2014). Climate Change: Synthesis Report. *Contribution of Working Groups I, II and III to the Fifth Assessment Report of the Intergovernmental Panel on Climate Change, IPCC*.
- Poling, E. B., Prausnitz, J. M. and Connell, J. P. O. (2001). The Properties of Gases and Liquids: **5th**: 803.
- Suleman, H.; Maulud, A. S.; Fosbøl, P. L.; Nasir, Q.; Nasir, R.; Shahid, M. Z.; Nawaz, M. and Abunowara, M. (2020). A Review of Semi-Empirical Equilibrium Models for CO₂-Alkanolamine-H₂O Solutions and their Mixtures at High Pressure. *Jour. Envir. Chem. Eng.*, **9**: 104713.
- Sun, P.; Grace, J. R.; Jim Lim, C. and Anthony, E. J. (2008a) Determination of Intrinsic Rate Constants of the CaO-CO₂ Reaction. *Chem. Eng. Scie.*, **63**: 47-56.
- Sun, P.; Grace, J. R.; Jim Lim, C. and Anthony, E. J. (2008b). A Discrete-pore Size Distribution-Based Gas Solid Model and its Application to the CaO with CO₂ Reaction. *Chem. Eng. Scie.*, **63**: 57-70.
- Szekely, J.; Evans, J. W. and Sohn, H. Y. (1976). Gas Solid Reactions. *Academic Press, London*: 612.
- Yagi, S. and Kunii, D. (1955). Studies on Combustion of Carbon Particles in Flames and Fluidized Beds. In: *5th International Symposium on Combustion*, Reinhold New York, USA: 231.
- Yagi, S., Kunii, D. (1961). *Chem. Chem Engi. Japan* **V**, **19**: 500p.

ABOUT THE AUTHORS



Mustafa A. Abunowara had a PhD., MSc, BSc in Chemical Engineering. He was working for Libyan Petroleum Institute from 2004 to 2012.
e-mail: abunowara1980@gmail.com



Mohamed Elgarni is a senior process engineer working in Canadian Natural Resources Limited (CNRL). He holds a PH.D. in Chemical Engineering from University of Wales. He has wealth of knowledge and experience in both field work and process modeling, simulation and troubleshooting of hydrotreaters and hydrogen plants. He has been actively involved in the development of multiple studies & projects related to upgrading of oil streams and utilities including GHG mitigation. Dr. Elgarni has in-depth experience in process design and operation in pilot and fully commercialized scale. He has worked for over 30 years in the oil & gas industry in plant operation, and research & development in the refining and oil production.
e-mail: mohamed.elgarni@cnrl.com